Published for SISSA by Springer

Received: *February 16, 2018*
Revised: *September 1, 2018*
Accepted: *September 3, 2018*
Published: *September 13, 2018*

Type II Seesaw and tau lepton at the HL-LHC, HE-LHC and FCC-hh

Tong Li

School of Physics, Nankai University,
94 Weijin Road, Tianjin, China

E-mail: nklitong@hotmail.com

Abstract: The tau lepton plays important role in distinguishing neutrino mass patterns and determining the chirality nature in heavy scalar mediated neutrino mass models, in the light of the neutrino oscillation experiments and its polarization measurement. We investigate the lepton flavor signatures with tau lepton at LHC upgrades, i.e. HL-LHC, HE-LHC and FCC-hh, through leptonic processes from doubly charged Higgs in the Type II Seesaw. We find that for the channel with one tau lepton in final states, the accessible doubly charged Higgs mass at HL-LHC can reach 655 GeV and 695 GeV for the neutrino mass patterns of normal hierarchy (NH) and inverted hierarchy (IH) respectively, with the luminosity of 3000 fb^{-1}. Higher masses, 975–1930 GeV for NH and 1035–2070 GeV for IH, can be achieved at HE-LHC and FCC-hh.

Keywords: Beyond Standard Model, Neutrino Physics

ArXiv ePrint: 1802.00945

https://doi.org/10.1007/JHEP09(2018)079

JHEP09(2018)079

Contents

1 Introduction

It is well-known that, in the context of the Standard Model (SM), the small but non-zero Majorana neutrino masses can be realized at leading order through a dimension-5 operator [1]

$$\frac{\kappa}{\Lambda} l_L l_L H H \tag{1.1}$$

where l_L and H stand for the SM lepton doublet and the Higgs doublet, respectively. Among the only three ultraviolet completions of eq. (1.1) at tree level, known as the Type I, Type II and Type III Seesaw mechanisms, the Type II Seesaw introduces an SU(2) Higgs triplet Δ and the consequent doubly charged Higgs ($H^{\pm\pm}$) decays with the violation of lepton number after the electroweak symmetry breaking (EWSB) [2–6]. If the lepton number violation happens at TeV scale, the Seesaw mechanism holds in terms of a relevant small coupling of the dimension-5 operator [7, 8] and the new Higgs states can be experimentally accessible at the Large Hadron Collider (LHC) [11–21].[1] Up to now, no significant evidence of doubly charged Higgs was observed at the LHC and thus the lower limit on doubly charged Higgs mass ($M_{H^{\pm\pm}}$) emerged. Assuming the branching fraction of $H^{\pm\pm}$ decay into same sign dilepton to be BR($H^{\pm\pm} \to \ell^{\pm}\ell^{\pm}$) = 100% and 10%, the most stringent lower mass limit by ATLAS is 770–870 GeV and 450 GeV respectively [22], with 36.1 fb^{-1} of integrated luminosity at 13 TeV LHC.

The relevant signal regions analyzed by ATLAS were defined by the combination of electron and/or muon final states. In other words, ATLAS only considered the decays of $H^{\pm\pm}$ such as $H^{\pm\pm} \to e^{\pm}e^{\pm}$, $\mu^{\pm}\mu^{\pm}$ or $e^{\pm}\mu^{\pm}$. It was emphasized that, however, governed by the constraints from neutrino oscillation experiments, the channels with tau lepton in doubly charged Higgs decays play an important role in distinguishing neutrino mass

[1] For recent review on TeV seesaw see e.g. refs. [9, 10] and references therein.

JHEP09(2018)079

hierarchies and determining mixing parameters [9, 10, 23, 24]. By contrast to ATLAS, CMS recently performed doubly charged Higgs search using events with tau lepton at the center-of-mass energy of 13 TeV with 12.9 fb^{-1} luminosity [25]. The lower bound on the $H^{\pm\pm}$ mass was reported to be about 481-537 (396) GeV assuming $\text{BR}(H^{\pm\pm} \to \tau^{\pm}\ell^{\pm}(\tau^{\pm}\tau^{\pm})) = 100\%$. In the CMS search and relevant studies [26], hadronic tau leptons were reconstructed without considering their polarization as chirality does not play any role in their analyses. The tau leptons before decay are considered to be tagged by a geometrical method.

Actually, the measurement of chirality in doubly charged Higgs search with tau lepton is important as it can help to discriminate different heavy scalar mediated neutrino mass mechanisms in which the doubly charged Higgs can couple to either left-handed or right-handed leptons. For example, H^{--} from an $\text{SU}(2)_L$ triplet field in the Type II Seesaw model only couples to left-handed charged leptons, while the one from an $\text{SU}(2)_L$ singlet field in the Zee-Babu model [27–29] only interacts with right-handed charged leptons. Without the chirality measurement in doubly charged Higgs search, it is impossible to discriminate these models except for their different production cross sections [22, 26]. Fortunately, it was pointed out that the chiral properties of the doubly charged Higgs Yukawa interactions can be determined by looking at the distributions of tau leptons' decay products [30]. Hence, it is necessary to investigate the search for doubly charged Higgs at colliders taking into account of both the neutrino oscillation constraints and the tau polarization.

Recently, several precise reactor measurements lead to more accurate lepton flavor predictions about the Seesaw models. For instance, Double Chooz [31], RENO [32] and in particular Daya Bay [33], have reported non-zero measurements of θ_{13} by looking for the disappearance of anti-electron neutrino. T2K and NOvA reported on indications of a non-zero leptonic CP phase [34–36]. These experiments provide us up-to-date neutrino oscillation results to investigate the impact on neutrino Seesaw models and consequently examine the lepton flavor signatures to be searched at colliders. Moreover, tau decay packages like Tauola [37–39] and more recent Taudecay [40] were developed to handle tau lepton decay. Thus, a detailed assessment of the search sensitivity is timely in order to seriously consider the channels with tau lepton from the experimental point of view, at the LHC upgrades such as the High-Luminosity LHC (HL-LHC) and the Higher-Energy LHC (HE-LHC) and the future 100 TeV pp circular collider (FCC-hh).

This work focuses on the search potential of doubly charged Higgs through tau channels in Type II seesaw, rather than distinguishing Type II seesaw and Zee-Babu model. We consider the tau channels followed by tau hadronic decay, because of the implications of neutrino oscillation data and tau polarization. The collider search for Zee-Babu model was recently studied in details in ref. [29]. The leptonic signatures in Zee-Babu model are very similar to those in Type II seesaw when new exotic particle channel is not kinematically allowed, but with different chirality of doubly charged Higgs and the consequent tau polarization.

This paper is organized as follows. In section 2, we first outline the Type II Seesaw model, discuss the constraints from neutrino oscillation experiments and show different doubly charged Higgs decay patterns. Then we simulate the production of doubly charged Higgs and its lepton number violating decays with tau lepton(s) in the final states at the

JHEP09(2018)079

LHC. The results of projected search for doubly charged Higgs search using tau lepton at HL-LHC, HE-LHC, and FCC-hh are given in section 3. Finally, in section 4 we summarize our conclusions.

2 Type II Seesaw with tau lepton at the LHC

2.1 Type II Seesaw model

We first review the lepton flavor physics in the Type II Seesaw mechanism. In Type II Seesaw an $SU(2)_L$ scalar triplet $\Delta \sim (1,3,1)$ which can be decomposed as

$$\Delta = \begin{pmatrix} \delta^+/\sqrt{2} & \delta^{++} \\ \delta^0 & -\delta^+/\sqrt{2} \end{pmatrix} \tag{2.1}$$

interacts with SM lepton doublet l_L through a Yukawa coupling Y_ν

$$Y_\nu \; l_L^T \; C \; i\sigma_2 \; \Delta \; l_L + h.c.\,, \tag{2.2}$$

and it also couples with the SM Higgs doublet H via the mixing term

$$\mu H^T \; i\sigma_2 \; \Delta^\dagger H + h.c.\,. \tag{2.3}$$

The neutrino mass is then given by

$$M_\nu = \sqrt{2} Y_\nu v_\Delta, \quad v_\Delta = \frac{\mu v_0^2}{\sqrt{2} M_\Delta^2}\,, \tag{2.4}$$

with M_Δ being the mass of the heavy triplet Higgs, and v_0 and v_Δ are the vevs of the neutral component of the Higgs doublet and triplet respectively satisfying $v_0^2 + v_\Delta^2 \approx (246\text{ GeV})^2$. As a result, the lepton number is broken by Δ spontaneously. After the electroweak symmetry breaking, there are seven physical Higgses, including the singly charged Higgs $H^\pm \approx \delta^\pm$ and doubly charged Higgs $H^{\pm\pm} = \delta^{\pm\pm}$ with $M_{H^\pm} = M_{H^{\pm\pm}} = M_\Delta$. The Yukawa interactions of the doubly charged Higgs are

$$\ell_L^T \; C \; Y_\nu^{++} \; H^{++} \; \ell_L, \qquad Y_\nu^{++} = \frac{M_\nu}{\sqrt{2} v_\Delta} = U_{PMNS}^* \; \frac{m_\nu^{\text{diag}}}{\sqrt{2}\; v_\Delta} \; U_{PMNS}^\dagger, \tag{2.5}$$

with U_{PMNS} being the Pontecorvo-Maki-Nakagawa-Sakata (PMNS) neutrino mixing matrix and the partial width of doubly charged Higgs decay into same-sign leptons is thus given by

$$\Gamma(H^{++} \to \ell_i^+ \ell_j^+) = \frac{1}{4\pi(1+\delta_{ij})} |(Y_\nu^{++})_{ij}|^2 M_{H^{++}}. \tag{2.6}$$

Note that below $v_\Delta \approx 10^{-4}\,\text{GeV}$, the decays of doubly charged Higgs H^{++} are dominated by the above lepton number violating channels [23, 24]. To focus on the same-sign leptonic decay modes of H^{++}, we assume $v_\Delta \lesssim 10^{-4}\,\text{GeV}$ in the analysis below. The decay branching ratios are only governed by eq. (2.6) and thus independent of $M_{H^{++}}$.

JHEP09(2018)079

In order to understand the implication of the neutrino experiments, we then discuss the neutrino mass and mixing parameters in the light of oscillation data. The neutrino mixing matrix can be parameterized as

$$U_{PMNS} = \begin{pmatrix} c_{12}c_{13} & c_{13}s_{12} & e^{-\mathrm{i}\delta}s_{13} \\ -c_{12}s_{13}s_{23}e^{\mathrm{i}\delta} - c_{23}s_{12} & c_{12}c_{23} - e^{\mathrm{i}\delta}s_{12}s_{13}s_{23} & c_{13}s_{23} \\ s_{12}s_{23} - e^{\mathrm{i}\delta}c_{12}c_{23}s_{13} & -c_{23}s_{12}s_{13}e^{\mathrm{i}\delta} - c_{12}s_{23} & c_{13}c_{23} \end{pmatrix} \times \mathrm{diag}(e^{i\Phi_1/2}, 1, e^{i\Phi_2/2}) \tag{2.7}$$

where $s_{ij} \equiv \sin\theta_{ij}$, $c_{ij} \equiv \cos\theta_{ij}$, $0 \leq \theta_{ij} \leq \pi/2$ and $0 \leq \delta, \Phi_i \leq 2\pi$ with δ being the Dirac CP phase and Φ_i the Majorana phases. The size of the mass-squared splitting between three neutrino states is extracted from neutrino oscillation experiments. The sign of $\Delta m^2_{31} = m^2_3 - m^2_1$, however, still remains unknown, which can be either positive, the Normal Hierarchy (NH), or negative, the Inverted Hierarchy (IH), for the spectrum of the neutrino masses.

Taking into account the reactor data from the antineutrino disappearance experiments mentioned above together with other disappearance and appearance results, the latest global fit of the neutrino masses and mixing parameters, at 3σ level [41, 42], are listed here

$$\begin{aligned} 6.8 \times 10^{-5}\,\mathrm{eV}^2 &< \Delta m^2_{21} < 8.02 \times 10^{-5}\,\mathrm{eV}^2, \\ 2.399 \times 10^{-3}\,\mathrm{eV}^2 &< \Delta m^2_{31} < 2.593 \times 10^{-3}\,\mathrm{eV}^2, \\ (-2.562 \times 10^{-3}\,\mathrm{eV}^2 &< \Delta m^2_{32} < -2.369 \times 10^{-3}\,\mathrm{eV}^2), \\ 0.272 &< \sin^2\theta_{12} < 0.346, \\ 0.418\ (0.435) &< \sin^2\theta_{23} < 0.613\ (0.616), \\ 0.01981\ (0.02006) &< \sin^2\theta_{13} < 0.02436\ (0.02452), \\ 144^\circ\ (192^\circ) &< \delta_{\mathrm{CP}} < 374^\circ(354^\circ), \end{aligned} \tag{2.8}$$

for NH (IH). We also adopt the tightest constraint on the sum of neutrino masses by combining the Planck+WMAP+highL+BAO data [43] at 95% confidence level (CL),

$$\sum_{i=1}^{3} m_i < 0.230\ \mathrm{eV}. \tag{2.9}$$

We then use the decay width formula in eq. (2.6) and vary the light neutrino masses, mixing angles and CP phase in the regions given in eqs. (2.8) and (2.9). The allowed values for different doubly charged Higgs decay patterns can be obtained for NH and IH below. One can see that the results are considerably improved compared to the old ones in refs. [23, 24].

For simplicity, we ignore the effects of the Majorana phases, i.e. $\Phi_1 = \Phi_2 = 0$ in eq. (2.7). In the case of the decays into two identical leptons as shown in figure 1 (a, b), in the NH case, the branching fraction of $\mathrm{BR}(H^{++} \to \tau^+\tau^+)$ is comparable to that of $\mu^+\mu^+$ channel and differs from $\mathrm{BR}(H^{++} \to e^+e^+)$ by two orders of magnitude. In the neutrino mass pattern of IH, the branching ratios of $e^+e^+, \mu^+\mu^+, \tau^+\tau^+$ channels remain in the same order. For both spectra in the case of the decays with different lepton flavors in the final states, $H^{++} \to \tau^+\mu^+$ is always dominant with at least one order of magnitude larger

JHEP09(2018)079

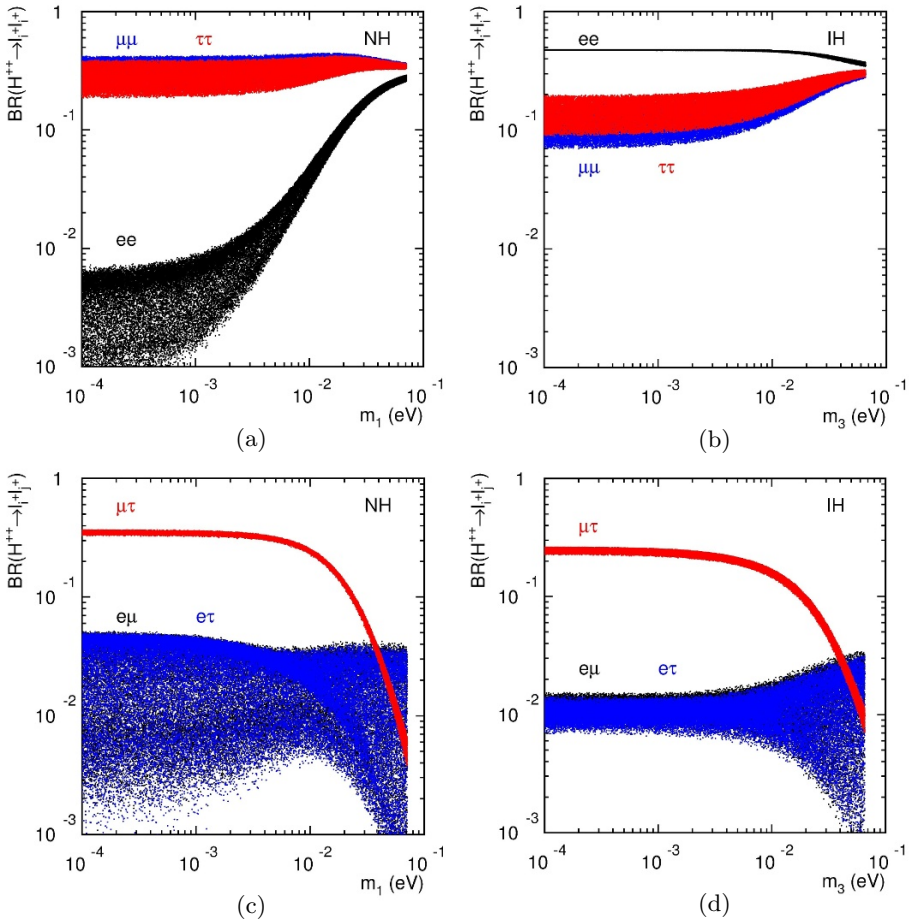

Figure 1. Scatter plots for the H^{++} decay branching fractions to the flavor-diagonal (a, b) and flavor-off-diagonal (c, d) like-sign dileptons versus the lowest neutrino mass for NH (a, c) and IH (b, d) with $\Phi_1 = \Phi_2 = 0$.

BR	ee	$e\mu$	$e\tau$	$\mu\mu$	$\mu\tau$	$\tau\tau$
NH	0	2.5%	2.5%	30%	35%	30%
IH	50%	1%	1%	12%	24%	12%

Table 1. Benchmark decay branching ratios of doubly charged Higgs for NH and IH spectra.

branching ratio, compared to $e^+\mu^+, e^+\tau^+$ as shown in figure 1 (c, d). In our numerical calculations below, we take two benchmarks of doubly charged Higgs decay branching ratios for NH and IH, as shown in table 1. They are consistent with the scatter plots in figure 1.

2.2 Testing Type II Seesaw with tau lepton at the LHC

The most appealing production at hadron colliders for triplet Higgs bosons is the pair production of doubly charged Higgs

$$pp \to Z^*/\gamma^* \to H^{++}H^{--} \tag{2.10}$$

JHEP09(2018)079

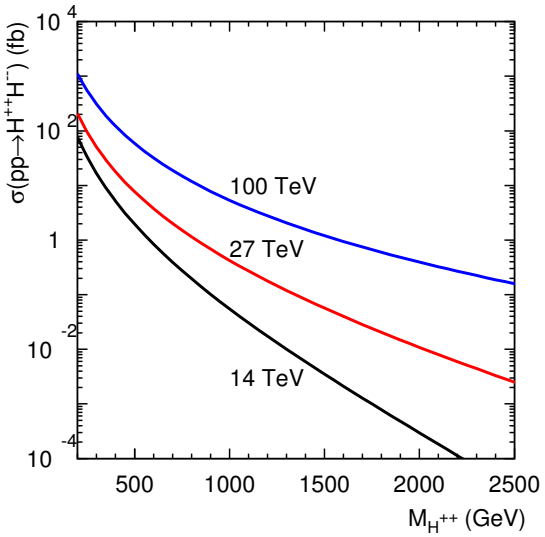

Figure 2. The total cross section of $pp \to H^{++}H^{--}$ with collision energy of 14 TeV, 27 TeV and 100 TeV.

followed by lepton number violating decays as discussed in last section. One crucial difference in the production process between Type II Seesaw and Zee-Babu model is the associated production of doubly and singly charged Higgses which only appears in Type II Seesaw. The bounds on the doubly charged Higgs mass from the associated production are stronger for the triplet case [25]. We show the total cross section of $pp \to H^{++}H^{--}$ with collision energy of 14 TeV, 27 TeV and 100 TeV respectively, through $q\bar{q}$ annihilation, and apply an overall next-to-leading (NLO) QCD K-factor of 1.25 below [44]. The main backgrounds come from diboson and $t\bar{t}X$ channels [22]. Without loss of generality, we choose ZZ and $t\bar{t}Z$ events to estimate our background contribution as they produce irreducible background source. With NLO in QCD their cross sections are $\sigma(ZZ) = 14.4 \pm 0.1$ pb and $\sigma(t\bar{t}Z) = 0.664 \pm 0.006$ pb at 14 TeV LHC using MadGraph5_aMC@NLO [45]. LNV-Scalars_UFO [26] is interfaced with MadGraph5 to generate signal events. We also use Taudecay_UFO [40] to simulate tau lepton decay carrying polarization information at parton level. Note that the coupling of the doubly charged Higgs to Z boson is $g\frac{1-2s_W^2}{c_W}$ and $g\frac{-2s_W^2}{c_W}$ in the $\mathrm{SU}(2)_L$ triplet and singlet case, respectively [26]. The mass bound on $M_{H^{\pm\pm}}$ is 500–600 GeV from the observed limits by CMS [25], given the realistic decay branching ratios as shown in table 1. Thus, we show the kinematics of tau channels with $M_{H^{\pm\pm}} = 800$ GeV below.

2.2.1 $H^{++}H^{--} \to \tau^{\pm}\ell^{\pm}\ell^{\mp}\ell^{\mp}$

The first signal channel we consider is the pair production of doubly charged Higgs with one tau lepton in the subsequent decays: $pp \to H^{++}H^{--} \to \tau^{\pm}\ell^{\pm}\ell^{\mp}\ell^{\mp}$. Note that we adopt the τ's leading 2-body decay channel, i.e. $\tau^{\pm} \to \pi^{\pm}\overset{(-)}{\nu}_{\tau}$, with the branching fraction being $\mathrm{BR}(\tau^{\pm} \to \pi^{\pm}\overset{(-)}{\nu}_{\tau}) = 0.11$. The τ-spin correlation is maximized in this decay channel.

JHEP09(2018)079

The major SM backgrounds are thus from

- ZZ diboson events with one Z decaying to charged leptons $\ell = e, \mu$ and the other to tau lepton pairs. One tau in the pairs has hadronic 2-body decay and the other tau decays via 3-body leptonic decay mode, i.e. $\tau^\pm \to \ell^\pm \nu_\ell \nu_\tau$:

$$ZZ \to \ell^+\ell^-\tau^+\tau^- \to \ell^+\ell^-\ell^\mp\pi^\pm + \nu's. \tag{2.11}$$

- $t\bar{t}Z$ events with Z boson decaying to charged leptons $\ell = e, \mu$. The W boson from one top quark leptonically decays to $\ell^\pm\nu$ and the other W is followed by decay to tau lepton and tau's hadronic decay:

$$t\bar{t}Z_{\to\ell^+\ell^-} \to b\bar{b}\tau^\pm\ell^\mp\ell^+\ell^- + 2\nu \to b\bar{b}\pi^\pm\ell^\mp\ell^+\ell^- + \nu's. \tag{2.12}$$

- $t\bar{t}Z$ events with $Z \to \tau^+\tau^-$ and the W bosons' leptonic decay from two top quarks. The subsequent channels of the tau leptons are respectively through the 2-body hadronic decay and the 3-body leptonic decay as above:

$$t\bar{t}Z_{\to\tau^+\tau^-} \to b\bar{b}\ell^+\ell^-\tau^+\tau^- + 2\nu \to b\bar{b}\ell^+\ell^-\pi^\pm\ell^\mp + \nu's. \tag{2.13}$$

We select events wtih three of the first two generation charged leptons $\ell = e, \mu$ and one hadronically decaying τ lepton. The three ℓ leptons are composed of two same-sign and one opposite-sign leptons. They and the decay product $\pi^\pm$ from tau should satisfy the following basic cuts [22, 25]:

$$p_T(\ell) \geq 15 \text{ GeV},\ |\eta(\ell)| < 2.5;\ p_T(\pi) \geq 20 \text{ GeV},\ |\eta(\pi)| < 2.3;\ \Delta R_{\ell\pi}, \Delta R_{\ell\ell} \geq 0.4. \tag{2.14}$$

In figure 3 we display the distributions of signal (assuming $M_{H^{\pm\pm}} = 800\,\text{GeV}$) and backgrounds at the 14 TeV LHC after the basic cuts shown in eq. (2.14), for (a) transverse momentum for the hardest ℓ lepton, (b) transverse pion momentum $p_T(\pi)$ and (c) missing transverse energy $\not{E}_T$. As the three ℓ leptons are from the decay of heavy doubly charged Higgs in our signal, we tighten the selection cuts by imposing:

$$p_T^{\max}(\ell) > M_{H^{\pm\pm}}/2. \tag{2.15}$$

This is from a smeared-out distribution of our signal around the Jacobean peak at $p_T(\ell) \sim M_{\ell^\pm\ell^\pm}/2$. Furthermore, the signal also has a harder $p_T(\pi)$ spectrum compared to the background. We thus strengthen their transverse momenta and the missing transverse energy induced by tau decay:

$$p_T(\pi),\ \not{E}_T > M_{H^{\pm\pm}}/30 + 40 \text{ GeV}. \tag{2.16}$$

Note that, for the H^{--} from an $\text{SU}(2)_L$ singlet field coupled only with right-handed tau lepton τ_R^-, the right-handed τ decays to a left-handed ν_τ, causing the π^- to preferentially move along the τ^- momentum direction. In contrast, the τ^- coming from a triplet H^{--} decay is left-handed which has the opposite effect on the π^-. The similar feature holds

JHEP09(2018)079

1τ efficiencies	basic cuts	p_T^ℓ	$p_T^\pi + \not{E}_T$	Z veto	$M_{\ell^\pm\ell^\pm}$
$H^{++}H^{--}(800)$	0.762	0.726	0.503	0.5021	0.5021
$\kappa^{++}\kappa^{--}(800)$	0.847	0.808	0.505	0.504	0.504
ZZ (800)	0.07	4.8×10^{-5}	2.7×10^{-5}	$< 1 \times 10^{-6}$	$< 1 \times 10^{-6}$
$(t\bar{t}Z)_1$ (800)	0.195	0.0017	5.38×10^{-4}	2.9×10^{-5}	1×10^{-6}
$(t\bar{t}Z)_2$ (800)	0.1685	4.1×10^{-4}	1.6×10^{-4}	1.5×10^{-4}	$< 1 \times 10^{-6}$

Table 2. The cut efficiencies for 1τ signal ($pp \to H^{++}H^{--} \to \tau^\pm\ell^\pm\ell^\mp\ell^\mp$) and the SM backgrounds after accumulated cuts with $\tau^\pm \to \pi^\pm \overset{(-)}{\nu}_\tau$ channel at the 14 TeV LHC. We assume $M_{H^{\pm\pm}} = 800\,\text{GeV}$. The efficiencies for the doubly charged Higgs $\kappa^{\pm\pm}$ in Zee-Babu model are also shown.

for the τ^+ from H^{++} decay. This is a well-known result of spin correlation in the τ decay [46, 47]. Thus, the transverse momentum of $\pi^\pm$ from doubly charged Higgs decay to tau lepton in Zee-Babu model yields a harder spectrum than that from Type II Seesaw, as seen in figure 3 (b). Because of the almost back-to-back same-sign dilepton from each doubly charged Higgs, the harder transverse momentum of pion yields a larger cancellation of all objects' momenta and thus a smaller missing energy as shown in figure 3 (c). The $p_T(\ell)$ spectrum and the invariant mass of the same-sign leptons are very similar between Type II Seesaw and Zee-Babu model.

Note that doubly charged Higgs emerges in many other models, such as the left-right symmetric model [48–52] and the Georgi-Machacek model [53, 54]. The tau polarization can only help to determine the chirality of the doubly charged Higgs in different models, if the leptonic channels are allowed. However, for instance, we are unable to use tau polarization to distinguish $\Delta_L^{\pm\pm}$ in both Type II Seesaw and left-right symmetric model, or the doubly charged Higgs in Zee-Babu model (denoted by $\kappa^{\pm\pm}$) and $\Delta_R^{\pm\pm}$ in left-right symmetric model. One should consider other features in specific models, for instance the Drell-Yan production of doubly charged Higgs via the new neutral gauge boson Z_R in left-right symmetric model or the fact that the doubly charged Higgs in the quintuplet Higgs states in Georgi-Machacek model has interactions only with the weak gauge bosons, but does not couple to SM fermions.

Both the ZZ and the 1st $t\bar{t}Z$ backgrounds have the opposite-sign lepton pairs $\ell^+\ell^-$ from Z boson decay and can thus be reduced by vetoing the invariant mass of opposite-sign leptons satisfying

$$|M_{\ell^+\ell^-} - M_Z| < 10\ \text{GeV}. \tag{2.17}$$

The invariant mass of the same-sign leptons after basic cuts is shown in figure 3 (d). One can further apply a doubly charged Higgs resonance window, i.e. $|M_{\ell^\pm\ell^\pm} - M_{H^{\pm\pm}}| < 0.1 M_{H^{\pm\pm}}$, to discover signal events. The $t\bar{t}Z$ backgrounds can also be reduced by vetoing extra b-jets and we find the backgrounds are at negligible level after these requirements.

Given the characteristic features of the signal and backgrounds discussed above, we can use the Gaussian method to calculate the significance

$$S/\sqrt{S+B} \tag{2.18}$$

JHEP09(2018)079

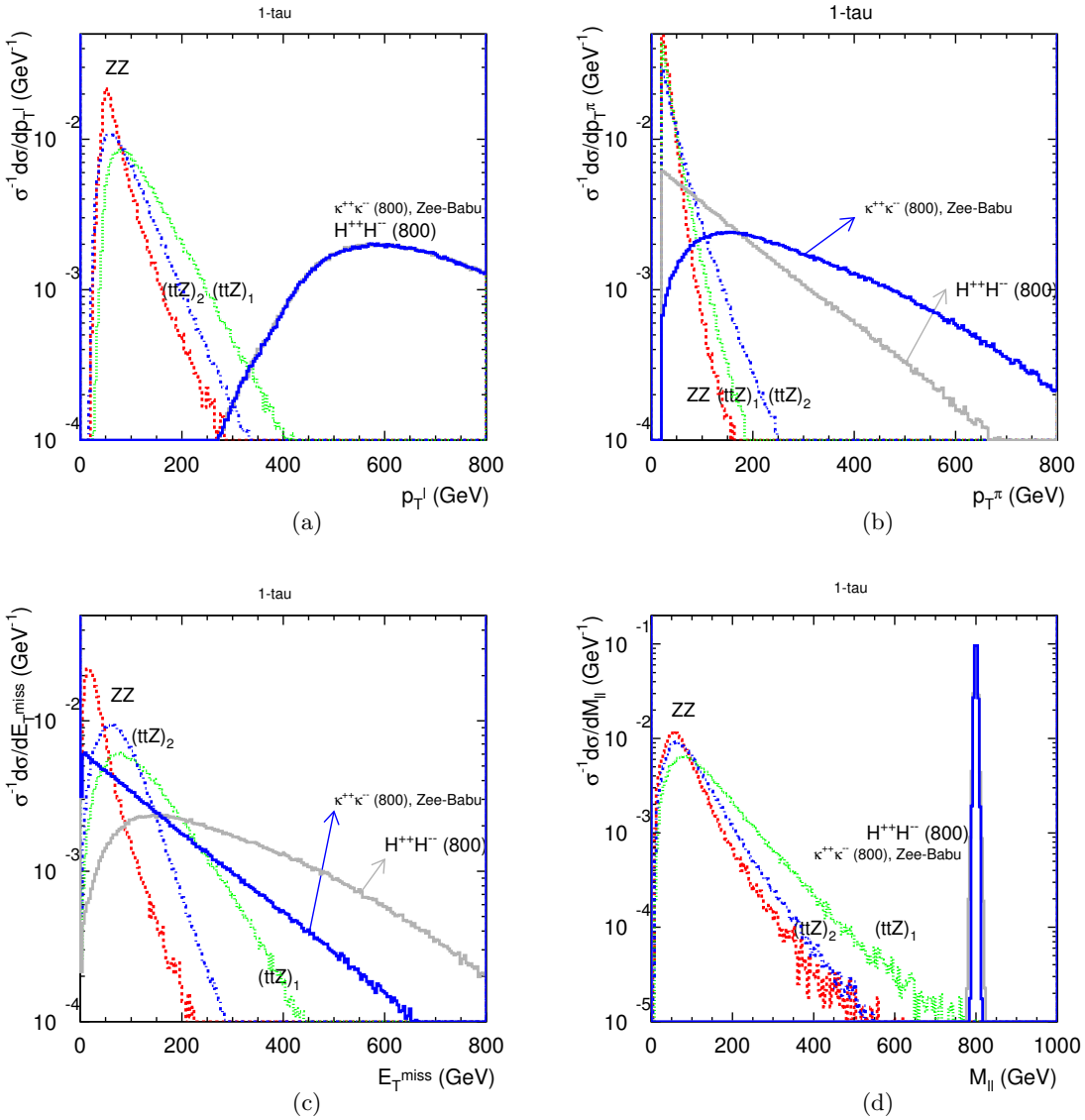

Figure 3. The normalized differential cross section distributions of signal $pp \to H^{++}H^{--} \to \tau^{\pm}\ell^{\pm}\ell^{\mp}\ell^{\mp}$ with $\tau^{\pm} \to \pi^{\pm}\overset{(-)}{\nu}_{\tau}$ and backgrounds versus (a) $p_T^{\max}(\ell)$, (b) $p_T(\pi)$, (c) $\not{E}_T$ and (d) $M_{\ell^{\pm}\ell^{\pm}}$ at the 14 TeV LHC. We assume $M_{H^{\pm\pm}} = 800\,\text{GeV}$. The distributions for the doubly charged Higgs $\kappa^{\pm\pm}$ in Zee-Babu model are also shown.

where S is the signal expectation and B is the sum of background expectations $B = \sum_{i=1,2,3} B_i$. With the proper branching fractions the discovered signal events for this channel read as

$$S = L \times \sigma(pp \to H^{++}H^{--}) \times \text{BR}(H^{++} \to \tau^+\ell^+) \times \text{BR}(H^{--} \to \ell^-\ell^-) \times 2 \times \\ \times \text{BR}(\tau^+ \to \pi^+\bar{\nu}_\tau) \times \epsilon^{1\tau}_{H^{\pm\pm}}, \tag{2.19}$$

JHEP09(2018)079

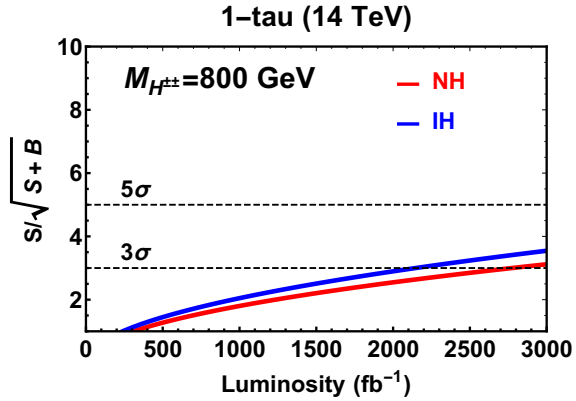

Figure 4. Significance of $pp \to H^{++}H^{--} \to \tau^{\pm}\ell^{\pm}\ell^{\mp}\ell^{\mp}$ with $\tau^{\pm} \to \pi^{\pm}\overset{(-)}{\nu}_{\tau}$ versus integrated luminosity (fb^{-1}) for NH and IH at 14 TeV LHC. We assume $M_{H^{\pm\pm}} = 800\,\text{GeV}$.

and the background expectations are

$$\begin{aligned}
B_1 &= L \times \sigma(pp \to ZZ) \times \text{BR}(Z \to \ell^+\ell^-) \times \text{BR}(Z \to \tau^+\tau^-) \times 2 \times \\
&\quad \times \text{BR}(\tau^+ \to \pi^+\bar{\nu}_\tau) \times \text{BR}(\tau^- \to \ell^-\nu_\tau\bar{\nu}_\ell) \times \epsilon^{1\tau}_{ZZ}, \\
B_2 &= L \times \sigma(pp \to t\bar{t}Z) \times \text{BR}(Z \to \ell^+\ell^-) \times \\
&\quad \times \text{BR}(W^+ \to \ell^+\nu_\ell) \times \text{BR}(W^- \to \tau^-\bar{\nu}_\tau) \times 2 \times \text{BR}(\tau^- \to \pi^-\nu_\tau) \times \epsilon^{1\tau}_{(t\bar{t}Z)_1}, \\
B_3 &= L \times \sigma(pp \to t\bar{t}Z) \times \text{BR}(Z \to \tau^+\tau^-) \times \text{BR}(W^+ \to \ell^+\nu_\ell) \times \text{BR}(W^- \to \ell^-\bar{\nu}_\ell) \times \\
&\quad \times 2 \times \text{BR}(\tau^+ \to \pi^+\bar{\nu}_\tau) \times \text{BR}(\tau^- \to \ell^-\nu_\tau\bar{\nu}_\ell) \times \epsilon^{1\tau}_{(t\bar{t}Z)_2},
\end{aligned} \tag{2.20}$$

where L is the integrated luminosity and the factor of 2 accounts for the charge-conjugation of final states. The $\epsilon^{1\tau}_{H^{\pm\pm}}, \epsilon^{1\tau}_{ZZ}, \epsilon^{1\tau}_{(t\bar{t}Z)_1}, \epsilon^{1\tau}_{(t\bar{t}Z)_2}$ denote the selection efficiencies for our signal with one tau and the relevant backgrounds, respectively, read from table 2. Figure 4 shows the significance versus integrated luminosity for NH and IH at 14 TeV LHC. For $M_{H^{\pm\pm}} = 800\,\text{GeV}$, the luminosity of 2800 (2150) fb^{-1} is required to reach 3σ significance for NH (IH). After all kinematic cuts, as seen in table 2, the signal selection efficiencies for Type II Seesaw and Zee-Babu model are very similar. Given the total production cross section in Type II Seesaw with an enhancement of 2.5 compared to Zee-Babu model, assuming the same decay branching ratios of doubly charged Higgs and certain luminosity, the significance for discovering Type II Seesaw is 1.6 times greater than Zee-Babu model.

2.2.2 $H^{++}H^{--} \to \ell^+\tau^+\ell^-\tau^-$

For the production of $H^{++}H^{--} \to \ell^+\tau^+\ell^-\tau^-$, we require that both tau leptons hadronically decay to charged pion and neutrino. The signal is thus composed of a pair of opposite-sign charged leptons and pions plus neutrinos, and the SM backgrounds are

$$ZZ \to \ell^+\ell^-\tau^+\tau^-,\ t\bar{t}Z_{\to\ell^+\ell^-} \to b\bar{b}\tau^+\tau^-\nu_\tau\bar{\nu}_\tau\ell^+\ell^-,\ t\bar{t}Z_{\to\tau^+\tau^-} \to b\bar{b}\ell^+\ell^-\nu_\ell\bar{\nu}_\ell\tau^+\tau^- \tag{2.21}$$

followed by $\tau^{\pm} \to \pi^{\pm}\overset{(-)}{\nu}_{\tau}$. We apply the same basic cuts as eq. (2.14) to the two pairs of opposite-sign ℓ lepton and charged pion in this channel.

JHEP09(2018)079

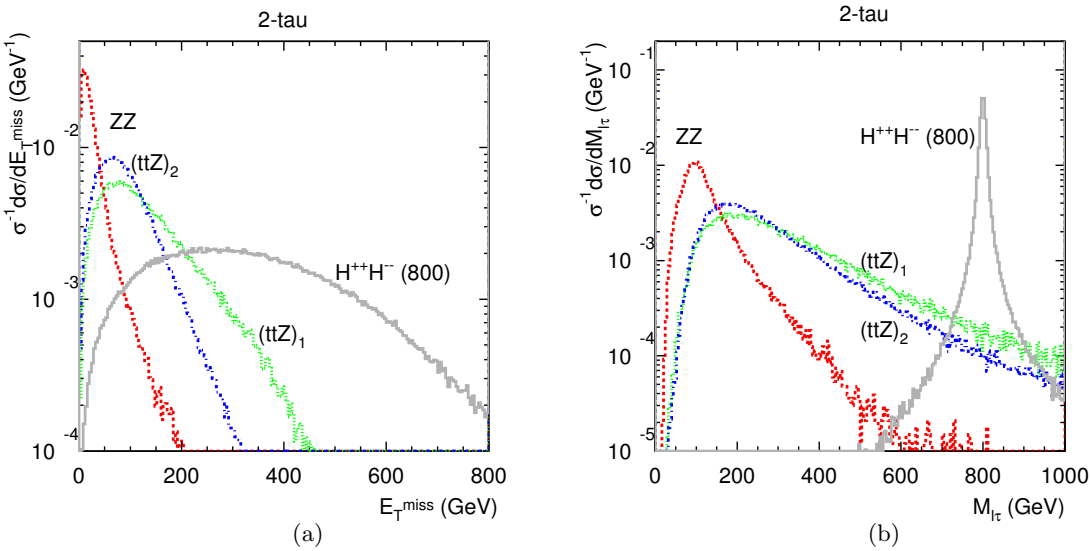

Figure 5. The normalized differential cross section distributions of signal $pp \to H^{++}H^{--} \to \ell^+\tau^+\ell^-\tau^-$ with $\tau^\pm \to \pi^\pm \overset{(-)}{\nu}_\tau$ and backgrounds versus (a) $\not{E}_T$ and (b) $M_{\ell^\pm\tau^\pm}$ at the 14 TeV LHC. We assume $M_{H^{\pm\pm}} = 800\,\text{GeV}$.

As seen from figure 5 (a), the missing energy is harder in this channel as there are more invisible neutrinos from tau decay. That is also why the kinematical reconstruction of the same-sign dilepton invariant mass is more complicated. Fortunately all the tau leptons are very energetic from the decay of a heavy doubly charged Higgs boson, the missing momentum of neutrinos will be along the direction with the charged track. We thus have

$$\vec{p}(\text{invisible}) = k_1\ \vec{p}(\text{track}_1) + k_2\ \vec{p}(\text{track}_2) \tag{2.22}$$

where k_1 and k_2 can be determined from the $\not{p}_T$ measurement. The tau and $H^{\pm\pm}$ Higgs pairs' kinematics can thus be fully reconstructed. The reconstructed Higgs mass from $\ell^\pm\tau^\pm$ is shown in figure 5 (b). One can see that the invariant mass is broader than that in the 1τ events. We thus modify the $\not{E}_T$ and mass window cut as below

$$\not{E}_T > M_{H^{\pm\pm}}/30 + 60\ \text{GeV} \quad \text{and} \quad |M_{\ell^\pm\tau^\pm} - M_{H^{\pm\pm}}| < 0.2 M_{H^{\pm\pm}}. \tag{2.23}$$

The rest selection requirements are the same as those in 1τ case.

The discovered signal events for this 2τ channel are

$$S = L \times \sigma(pp \to H^{++}H^{--}) \times \text{BR}^2(H^{\pm\pm} \to \tau^\pm\ell^\pm) \times \text{BR}^2(\tau^+ \to \pi^+\bar{\nu}_\tau) \times \epsilon^{2\tau}_{H^{\pm\pm}} \tag{2.24}$$

JHEP09(2018)079

2τ efficiencies	basic cuts	p_T^ℓ	$p_T^\pi + \not{E}_T$	Z veto	$M_{\ell^\pm\tau^\pm}$
$H^{++}H^{--}(800)$	0.67	0.51	0.454	0.454	0.45
ZZ (800)	0.0838	4.2×10^{-5}	3.4×10^{-5}	3×10^{-6}	$<1\times10^{-6}$
$(t\bar{t}Z)_1$ (800)	0.0733	6.93×10^{-4}	3.38×10^{-4}	2×10^{-5}	9×10^{-6}
$(t\bar{t}Z)_2$ (800)	0.1847	4×10^{-4}	2.52×10^{-4}	2.51×10^{-4}	7.57×10^{-5}

Table 3. The cut efficiencies for 2τ signal ($pp \to H^{++}H^{--} \to \ell^+\tau^+\ell^-\tau^-$) and the SM backgrounds after accumulated cuts with $\tau^\pm \to \pi^\pm \overset{(-)}{\nu}_\tau$ channel at the 14 TeV LHC. We assume $M_{H^{\pm\pm}} = 800\,\text{GeV}$.

and those for backgrounds are

$$\begin{aligned}
B_1 &= L\times\sigma(pp\to ZZ)\times \text{BR}(Z\to\ell^+\ell^-)\times \text{BR}(Z\to\tau^+\tau^-)\times \\
&\quad\times\text{BR}^2(\tau^+\to\pi^+\bar{\nu}_\tau)\times\epsilon^{2\tau}_{ZZ}, \\
B_2 &= L\times\sigma(pp\to t\bar{t}Z)\times \text{BR}(Z\to\ell^+\ell^-)\times \text{BR}^2(W^\pm\to\tau^\pm\overset{(-)}{\nu}_\tau)\times \\
&\quad\times\text{BR}^2(\tau^+\to\pi^+\bar{\nu}_\tau)\times\epsilon^{2\tau}_{(t\bar{t}Z)_1}, \\
B_3 &= L\times\sigma(pp\to t\bar{t}Z)\times \text{BR}(Z\to\tau^+\tau^-)\times \text{BR}^2(W^\pm\to\ell^\pm\overset{(-)}{\nu}_\tau)\times \\
&\quad\times\text{BR}^2(\tau^+\to\pi^+\bar{\nu}_\tau)\times\epsilon^{2\tau}_{(t\bar{t}Z)_2},
\end{aligned} \tag{2.25}$$

where the $\epsilon^{2\tau}_{H^{\pm\pm}}, \epsilon^{2\tau}_{ZZ}, \epsilon^{2\tau}_{(t\bar{t}Z)_1}, \epsilon^{2\tau}_{(t\bar{t}Z)_2}$ are the cut efficiencies from table 3. For this channel, it is impossible to discover doubly charged Higgs heavier than 300 GeV at 14 TeV LHC with luminosity below $3000\,\text{fb}^{-1}$. Upgrades of the LHC are needed to probe the doubly charged Higgs with decay to tau lepton.

3 Results for the HL-LHC, HE-LHC and FCC-hh

In this section we show the results of projected sensitivity to leptonic processes with tau lepton in Type II Seesaw, at the high luminosity/energy upgrades of the LHC and the future FCC-hh. For the HE-LHC and FCC-hh, we require that the decay products of doubly charged Higgs satisfy the following basic cuts:

$$p_T(\ell) \geq 30\ \text{GeV},\ p_T(\pi) \geq 25\ \text{GeV};\ |\eta(\ell,\pi)| < 2.5;\ \Delta R_{\ell\pi}, \Delta R_{\ell\ell} \geq 0.4. \tag{3.1}$$

The rest of selection cuts are the same as above.

In figures 6, 7 and 8 we display the 3σ and 5σ significance in the plane of integrated luminosity versus doubly charged Higgs mass for $pp \to H^{++}H^{--} \to \tau^\pm\ell^\pm\ell^\mp\ell^\mp, \ell^+\tau^+\ell^-\tau^-$ at the 14 TeV LHC, 27 TeV LHC and 100 TeV FCC-hh, respectively. One can see that the 14 TeV LHC can probe H^{++} mass up to 365 (655) GeV and 485 (815) GeV with 5σ and 3σ significance respectively for NH through 1τ channel, assuming $L = 300\ (3000)\,\text{fb}^{-1}$, while for IH the masses of 395 (695) GeV and 515 (855) GeV can be achieved. Note that, as taking tau polarization effect into account through its hadronic decay product, our prediction would be more conservative than those LHC made. The discovery mass at the

JHEP09(2018)079

$M_{H^{\pm\pm}}$	14 TeV	27 TeV	100 TeV
1τ NH	365 (655)	525 (975)	960 (1930)
1τ IH	395 (695)	567 (1035)	1050 (2070)
2τ NH	—	— (410)	305 (805)
2τ IH	—	— (305)	— (609)

Table 4. The reachable doubly charged Higgs mass (in the unit of GeV) at 5σ significance for 1τ and 2τ channels and NH and IH neutrino mass patterns, at the 14 TeV LHC, 27 TeV LHC and FCC-hh. We assume $L = 300\ (3000)\,\text{fb}^{-1}$.

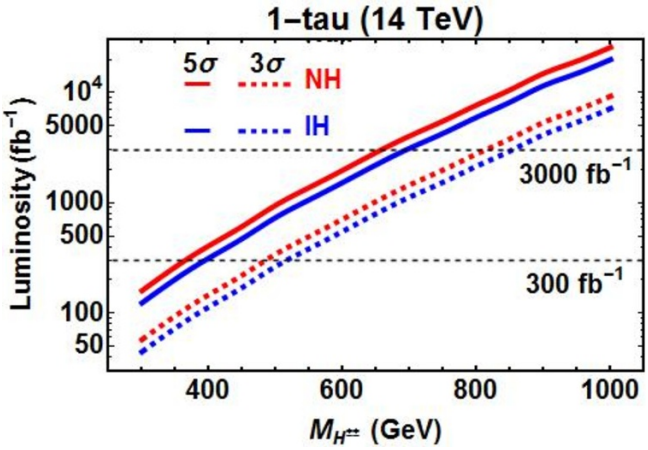

Figure 6. Integrated luminosity versus $M_{H^{\pm\pm}}$ at 3σ and 5σ significance for $pp \to H^{++}H^{--} \to \tau^{\pm}\ell^{\pm}\ell^{\mp}\ell^{\mp}$ with $\tau^{\pm} \to \pi^{\pm}\overset{(-)}{\nu}_{\tau}$ for NH and IH at 14 TeV LHC.

HE-LHC and FCC-hh is above 525 (975) GeV and 960 (1930) GeV respectively, for the luminosity of 300 (3000) fb^{-1}. The accessible mass for 2τ channel is much lower than 1τ channel, e.g. 300–400 GeV at HE-LHC and 600–800 GeV at FCC-hh.

Finally, we summarize the reachable doubly charged Higgs mass at 5σ significance for 1τ and 2τ channels and NH and IH neutrino mass patterns, at the 14 TeV LHC, 27 TeV LHC and 100 TeV FCC-hh, in table 4.

4 Conclusions

Neutrino oscillation measurements indicate that tau lepton plays manifest role in distinguishing different neutrino mass patterns. Moreover, tau polarization can help to determine the chiral property of its parent particle and thus discriminate different heavy scalar mediated neutrino mass mechanisms, such as Type II Seesaw and Zee-Babu model. We thus update the doubly charged Higgs decay patterns in Type II Seesaw in the light of the latest neutrino oscillation result and examine the lepton flavor signatures with tau lepton at LHC upgrades, i.e. HL-LHC, HE-LHC and FCC-hh, through leptonic processes from doubly charged Higgs in the Type II Seesaw. We investigate signal channels with both one and two tau leptons in final states from doubly charged Higgs pair production, i.e.

JHEP09(2018)079

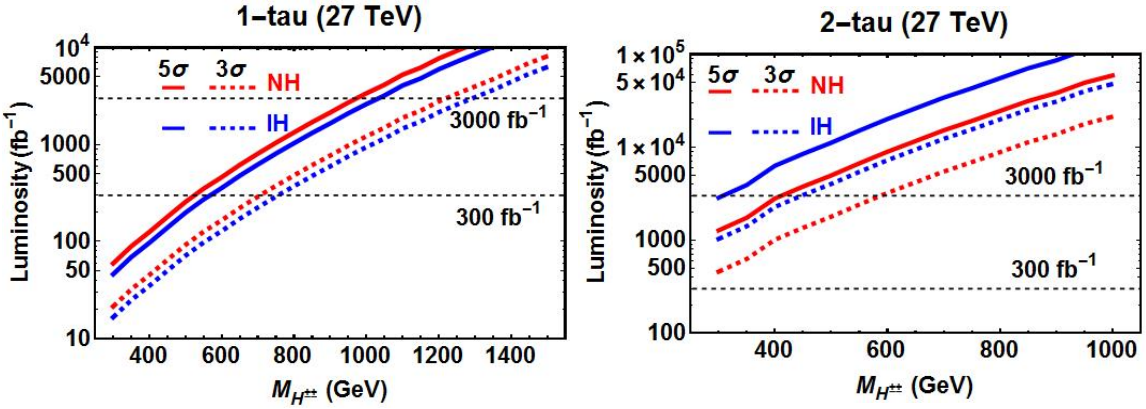

(a) (b)

Figure 7. Integrated luminosity versus $M_{H^{\pm\pm}}$ at 3σ and 5σ significance for $pp \to H^{++}H^{--} \to \tau^{\pm}\ell^{\pm}\ell^{\mp}\ell^{\mp}$ (a) and $\ell^{+}\tau^{+}\ell^{-}\tau^{-}$ (b) with $\tau^{\pm} \to \pi^{\pm}\overset{(-)}{\nu}_{\tau}$ for NH and IH at 27 TeV LHC.

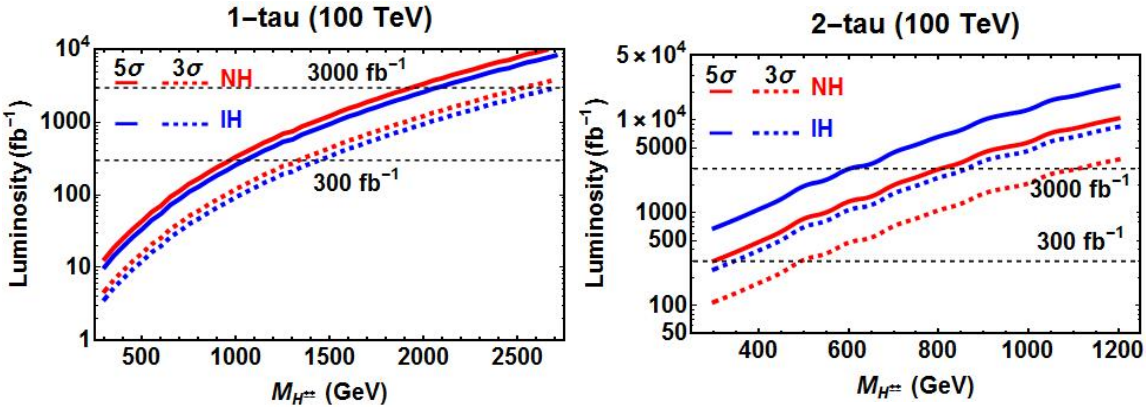

(a) (b)

Figure 8. Integrated luminosity versus $M_{H^{\pm\pm}}$ at 3σ and 5σ significance for $pp \to H^{++}H^{--} \to \tau^{\pm}\ell^{\pm}\ell^{\mp}\ell^{\mp}$ (a) and $\ell^{+}\tau^{+}\ell^{-}\tau^{-}$ (b) with $\tau^{\pm} \to \pi^{\pm}\overset{(-)}{\nu}_{\tau}$ for NH and IH at 100 TeV LHC.

$pp \to H^{++}H^{--} \to \tau^{\pm}\ell^{\pm}\ell^{\mp}\ell^{\mp}, \ell^{+}\tau^{+}\ell^{-}\tau^{-}$, and leading SM backgrounds with $\tau^{\pm} \to \pi^{\pm}\nu$. Although the importance of tau polarization for doubly charged Higgs was studied before [30], we alternatively point out that the polarization of tau lepton from doubly charged Higgs decay can be reflected in the p_T distribution of pion which is easier to measure.

With the analysis presented here we have found that, for the 1τ channel, the projected doubly charged Higgs mass at HL-LHC can reach 655 GeV and 695 GeV for NH and IH respectively with the luminosity of 3000 fb^{-1}. Higher masses, 975–1930 GeV for NH and 1035–2070 GeV for IH, can be achieved at HE-LHC and FCC-hh. The accessible mass for 2τ channel is much lower than that for 1τ channel.

Acknowledgments

The National Computational Infrastructure (NCI), the Southern Hemisphere's fastest supercomputer, is gratefully acknowledged.

JHEP09(2018)079

References

[1] S. Weinberg, *Baryon and lepton nonconserving processes*, *Phys. Rev. Lett.* **43** (1979) 1566 [INSPIRE].

[2] W. Konetschny and W. Kummer, *Nonconservation of total lepton number with scalar bosons*, *Phys. Lett.* **B 70** (1977) 433 [INSPIRE].

[3] T.P. Cheng and L.-F. Li, *Neutrino masses, mixings and oscillations in* SU(2) × U(1) *models of electroweak interactions*, *Phys. Rev.* **D 22** (1980) 2860 [INSPIRE].

[4] G. Lazarides, Q. Shafi and C. Wetterich, *Proton lifetime and fermion masses in an* SO(10) *model*, *Nucl. Phys.* **B 181** (1981) 287 [INSPIRE].

[5] J. Schechter and J.W.F. Valle, *Neutrino masses in* SU(2) × U(1) *theories*, *Phys. Rev.* **D 22** (1980) 2227 [INSPIRE].

[6] R.N. Mohapatra and G. Senjanović, *Neutrino masses and mixings in gauge models with spontaneous parity violation*, *Phys. Rev.* **D 23** (1981) 165 [INSPIRE].

[7] A. de Gouvêa, J. Jenkins and N. Vasudevan, *Neutrino phenomenology of very low-energy seesaws*, *Phys. Rev.* **D 75** (2007) 013003 [hep-ph/0608147] [INSPIRE].

[8] A. de Gouvêa, *GeV seesaw, accidentally small neutrino masses and Higgs decays to neutrinos*, arXiv:0706.1732 [INSPIRE].

[9] F.F. Deppisch, P.S. Bhupal Dev and A. Pilaftsis, *Neutrinos and collider physics*, *New J. Phys.* **17** (2015) 075019 [arXiv:1502.06541] [INSPIRE].

[10] Y. Cai, T. Han, T. Li and R. Ruiz, *Lepton number violation: seesaw models and their collider tests*, *Front. Phys.* **6** (2018) 40 [arXiv:1711.02180] [INSPIRE].

[11] A.G. Akeroyd and C.-W. Chiang, *Doubly charged Higgs bosons and three-lepton signatures in the Higgs triplet model*, *Phys. Rev.* **D 80** (2009) 113010 [arXiv:0909.4419] [INSPIRE].

[12] A.G. Akeroyd, C.-W. Chiang and N. Gaur, *Leptonic signatures of doubly charged Higgs boson production at the LHC*, *JHEP* **11** (2010) 005 [arXiv:1009.2780] [INSPIRE].

[13] A. Melfo, M. Nemevšek, F. Nesti, G. Senjanović and Y. Zhang, *Type II seesaw at LHC: the roadmap*, *Phys. Rev.* **D 85** (2012) 055018 [arXiv:1108.4416] [INSPIRE].

[14] B. Dutta, R. Eusebi, Y. Gao, T. Ghosh and T. Kamon, *Exploring the doubly charged Higgs boson of the left-right symmetric model using vector boson fusionlike events at the LHC*, *Phys. Rev.* **D 90** (2014) 055015 [arXiv:1404.0685] [INSPIRE].

[15] G. Bambhaniya, J. Chakrabortty, J. Gluza, T. Jelinski and R. Szafron, *Search for doubly charged Higgs bosons through vector boson fusion at the LHC and beyond*, *Phys. Rev.* **D 92** (2015) 015016 [arXiv:1504.03999] [INSPIRE].

[16] G. Bambhaniya, P.S.B. Dev, S. Goswami and M. Mitra, *The scalar triplet contribution to lepton flavour violation and neutrinoless double beta decay in left-right symmetric model*, *JHEP* **04** (2016) 046 [arXiv:1512.00440] [INSPIRE].

[17] K.S. Babu and S. Jana, *Probing doubly charged Higgs bosons at the LHC through photon initiated processes*, *Phys. Rev.* **D 95** (2017) 055020 [arXiv:1612.09224] [INSPIRE].

JHEP09(2018)079

[18] P.S.B. Dev, R.N. Mohapatra and Y. Zhang, *Probing the Higgs sector of the minimal left-right symmetric model at future hadron colliders*, *JHEP* **05** (2016) 174 [arXiv:1602.05947] [INSPIRE].

[19] Y. Sui and Y. Zhang, *Prospects of type-II seesaw models at future colliders in light of the DAMPE e^+e^- excess*, *Phys. Rev.* **D 97** (2018) 095002 [arXiv:1712.03642] [INSPIRE].

[20] M. Mitra, S. Niyogi and M. Spannowsky, *Type-II seesaw model and multilepton signatures at hadron colliders*, *Phys. Rev.* **D 95** (2017) 035042 [arXiv:1611.09594] [INSPIRE].

[21] P.S.B. Dev, C.M. Vila and W. Rodejohann, *Naturalness in testable type-II seesaw scenarios*, *Nucl. Phys.* **B 921** (2017) 436 [arXiv:1703.00828] [INSPIRE].

[22] ATLAS collaboration, *Search for doubly charged Higgs boson production in multi-lepton final states with the ATLAS detector using proton-proton collisions at $\sqrt{s} = 13$ TeV*, *Eur. Phys. J.* **C 78** (2018) 199 [arXiv:1710.09748] [INSPIRE].

[23] P. Fileviez Perez, T. Han, G.-Y. Huang, T. Li and K. Wang, *Testing a neutrino mass generation mechanism at the LHC*, *Phys. Rev.* **D 78** (2008) 071301 [arXiv:0803.3450] [INSPIRE].

[24] P. Fileviez Perez, T. Han, G.-Y. Huang, T. Li and K. Wang, *Neutrino masses and the CERN LHC: testing type II seesaw*, *Phys. Rev.* **D 78** (2008) 015018 [arXiv:0805.3536] [INSPIRE].

[25] CMS collaboration, *A search for doubly-charged Higgs boson production in three and four lepton final states at $\sqrt{s} = 13$ TeV*, CMS-PAS-HIG-16-036, CERN, Geneva, Switzerland, (2016).

[26] F. del Águila and M. Chala, *LHC bounds on lepton number violation mediated by doubly and singly-charged scalars*, *JHEP* **03** (2014) 027 [arXiv:1311.1510] [INSPIRE].

[27] A. Zee, *Quantum numbers of Majorana neutrino masses*, *Nucl. Phys.* **B 264** (1986) 99 [INSPIRE].

[28] K.S. Babu, *Model of 'calculable' Majorana neutrino masses*, *Phys. Lett.* **B 203** (1988) 132 [INSPIRE].

[29] J. Alcaide, M. Chala and A. Santamaria, *LHC signals of radiatively-induced neutrino masses and implications for the Zee-Babu model*, *Phys. Lett.* **B 779** (2018) 107 [arXiv:1710.05885] [INSPIRE].

[30] H. Sugiyama, K. Tsumura and H. Yokoya, *Discrimination of models including doubly charged scalar bosons by using tau lepton decay distributions*, *Phys. Lett.* **B 717** (2012) 229 [arXiv:1207.0179] [INSPIRE].

[31] DOUBLE CHOOZ collaboration, Y. Abe et al., *Indication of reactor $\bar{\nu}_e$ disappearance in the Double CHOOZ experiment*, *Phys. Rev. Lett.* **108** (2012) 131801 [arXiv:1112.6353] [INSPIRE].

[32] RENO collaboration, J.K. Ahn et al., *Observation of reactor electron antineutrino disappearance in the RENO experiment*, *Phys. Rev. Lett.* **108** (2012) 191802 [arXiv:1204.0626] [INSPIRE].

[33] DAYA BAY collaboration, F.P. An et al., *Observation of electron-antineutrino disappearance at Daya Bay*, *Phys. Rev. Lett.* **108** (2012) 171803 [arXiv:1203.1669] [INSPIRE].

[34] T2K collaboration, K. Abe et al., *Combined analysis of neutrino and antineutrino oscillations at T2K*, *Phys. Rev. Lett.* **118** (2017) 151801 [arXiv:1701.00432] [INSPIRE].

JHEP09(2018)079

[35] NOvA collaboration, P. Adamson et al., *First measurement of electron neutrino appearance in NOvA*, *Phys. Rev. Lett.* **116** (2016) 151806 [arXiv:1601.05022] [INSPIRE].

[36] T2K collaboration, K. Abe et al., *Observation of electron neutrino appearance in a muon neutrino beam*, *Phys. Rev. Lett.* **112** (2014) 061802 [arXiv:1311.4750] [INSPIRE].

[37] S. Jadach, J.H. Kuhn and Z. Was, *TAUOLA: a library of Monte Carlo programs to simulate decays of polarized tau leptons*, *Comput. Phys. Commun.* **64** (1990) 275 [INSPIRE].

[38] M. Jezabek, Z. Was, S. Jadach and J.H. Kuhn, *The tau decay library TAUOLA, update with exact $O(\alpha)$ QED corrections in $\tau \to \mu(e)\nu\bar{\nu}$ decay modes*, *Comput. Phys. Commun.* **70** (1992) 69 [INSPIRE].

[39] S. Jadach, Z. Was, R. Decker and J.H. Kuhn, *The tau decay library TAUOLA: version* 2.4, *Comput. Phys. Commun.* **76** (1993) 361 [INSPIRE].

[40] K. Hagiwara, T. Li, K. Mawatari and J. Nakamura, *TauDecay: a library to simulate polarized tau decays via FeynRules and MadGraph*5, *Eur. Phys. J.* **C 73** (2013) 2489 [arXiv:1212.6247] [INSPIRE].

[41] I. Esteban, M.C. Gonzalez-Garcia, M. Maltoni, I. Martinez-Soler and T. Schwetz, *Updated fit to three neutrino mixing: exploring the accelerator-reactor complementarity*, *JHEP* **01** (2017) 087 [arXiv:1611.01514] [INSPIRE].

[42] *NuFIT* 3.2, http://www.nu-fit.org, (2018).

[43] PLANCK collaboration, P.A.R. Ade et al., *Planck* 2015 *results. XIII. Cosmological parameters*, *Astron. Astrophys.* **594** (2016) A13 [arXiv:1502.01589] [INSPIRE].

[44] M. Muhlleitner and M. Spira, *A note on doubly charged Higgs pair production at hadron colliders*, *Phys. Rev.* **D 68** (2003) 117701 [hep-ph/0305288] [INSPIRE].

[45] J. Alwall et al., *The automated computation of tree-level and next-to-leading order differential cross sections and their matching to parton shower simulations*, *JHEP* **07** (2014) 079 [arXiv:1405.0301] [INSPIRE].

[46] B.K. Bullock, K. Hagiwara and A.D. Martin, *Tau polarization as a signal of charged Higgs bosons*, *Phys. Rev. Lett.* **67** (1991) 3055 [INSPIRE].

[47] B.K. Bullock, K. Hagiwara and A.D. Martin, *Tau polarization and its correlations as a probe of new physics*, *Nucl. Phys.* **B 395** (1993) 499 [INSPIRE].

[48] J.C. Pati and A. Salam, *Lepton number as the fourth color*, *Phys. Rev.* **D 10** (1974) 275 [*Erratum ibid.* **D 11** (1975) 703] [INSPIRE].

[49] R.N. Mohapatra and J.C. Pati, *Left-right gauge symmetry and an isoconjugate model of CP-violation*, *Phys. Rev.* **D 11** (1975) 566 [INSPIRE].

[50] R.N. Mohapatra and J.C. Pati, *A natural left-right symmetry*, *Phys. Rev.* **D 11** (1975) 2558 [INSPIRE].

[51] G. Senjanović and R.N. Mohapatra, *Exact left-right symmetry and spontaneous violation of parity*, *Phys. Rev.* **D 12** (1975) 1502 [INSPIRE].

[52] G. Senjanović, *Spontaneous breakdown of parity in a class of gauge theories*, *Nucl. Phys.* **B 153** (1979) 334 [INSPIRE].

[53] H. Georgi and M. Machacek, *Doubly charged Higgs bosons*, *Nucl. Phys.* **B 262** (1985) 463 [INSPIRE].

[54] M.S. Chanowitz and M. Golden, *Higgs boson triplets with $M_W = M_Z \cos\theta_\omega$*, *Phys. Lett.* **B 165** (1985) 105 [INSPIRE].

JHEP09(2018)079